

<https://helda.helsinki.fi>

Observation of Medium-Induced Modifications of Jet Fragmentation in Pb-Pb Collisions at $\sqrt{s(NN)}=5.02$ TeV Using Isolated Photon-Tagged Jets

The CMS collaboration

2018-12-14

The CMS Collaboration , Sirunyan , A M , Eerola , P , Kirschenmann , H , Pekkanen , J , Voutilainen , M , Havukainen , J , Heikkilä , J K , Järvinen , T , Karimäki , V , Kinnunen , R , Lampén , T , Lassila-Perini , K , Laurila , S , Lehti , S , Lindén , T , Luukka , P , Mäenpää , T , Siikonen , H , Tuominen , E , Tuominiemi , J & Tuuva , T 2018 , ' Observation of Medium-Induced Modifications of Jet Fragmentation in Pb-Pb Collisions at $\sqrt{s(NN)}=5.02$ TeV Using Isolated Photon-Tagged Jets ' , Physical Review Letters , vol. 121 , no. 24 , 242301 . <https://doi.org/10.1103/PhysRevLett.121.242301>

<http://hdl.handle.net/10138/289805>

<https://doi.org/10.1103/PhysRevLett.121.242301>

cc_by
publishedVersion

Downloaded from Helda, University of Helsinki institutional repository.

This is an electronic reprint of the original article.

This reprint may differ from the original in pagination and typographic detail.

Please cite the original version.

Observation of Medium-Induced Modifications of Jet Fragmentation in Pb-Pb Collisions at $\sqrt{s_{\text{NN}}} = 5.02$ TeV Using Isolated Photon-Tagged Jets

A. M. Sirunyan *et al.**
(CMS Collaboration)

 (Received 15 January 2018; revised manuscript received 16 October 2018; published 14 December 2018)

Measurements of fragmentation functions for jets associated with an isolated photon are presented for the first time in pp and Pb-Pb collisions. The analysis uses data collected with the CMS detector at the CERN LHC at a nucleon-nucleon center-of-mass energy of 5.02 TeV. Fragmentation functions are obtained for jets with $p_T^{\text{jet}} > 30$ GeV/ c in events containing an isolated photon with $p_T^\gamma > 60$ GeV/ c , using charged tracks with transverse momentum $p_T^{\text{trk}} > 1$ GeV/ c in a cone around the jet axis. The association with an isolated photon constrains the initial p_T and azimuthal angle of the parton whose shower produced the jet. For central Pb-Pb collisions, modifications of the jet fragmentation functions are observed when compared to those measured in pp collisions, while no significant differences are found in the 50% most peripheral collisions. Jets in central Pb-Pb events show an excess (depletion) of low (high) p_T particles, with a transition around 3 GeV/ c . This measurement shows for the first time the in-medium shower modifications of partons (quark dominated) with well-defined initial kinematics. It constitutes a new well-controlled reference for testing theoretical models of the parton passage through the quark-gluon plasma.

DOI: [10.1103/PhysRevLett.121.242301](https://doi.org/10.1103/PhysRevLett.121.242301)

A deconfined state of quarks and gluons, called the quark-gluon plasma (QGP) [1], is believed to be produced on a short timescale in high energy nucleus-nucleus collisions [2]. Occasionally, a pair of partons (quarks or gluons) in the colliding nuclei undergoes a high transverse momentum (p_T) scattering, a process that occurs over a shorter timescale. As they pass through and interact with the QGP, the scattered partons lose some of their energy [3–8]. The relative importance of the various mechanisms by which these partons lose energy to the medium has been a continuous focus of the field of relativistic heavy ion collisions [9–14].

The outgoing hard-scattered partons eventually fragment, and each forms a jet of collimated particles. The CERN LHC collaborations have conducted various (di)jet studies: modifications of the jet yield in the medium (jet quenching) [15–17], jet fragmentation functions (the probability for a parton to fragment into particles carrying a given fraction of the jet momentum) [18,19], missing p_T in dijet systems [20–22], jet-track correlations [23], and the radial p_T profile of tracks within jets [24]. However, in these analyses, the energy lost by the partons diminishes the information about their initial properties. One way to

overcome this challenge is to study processes in which the initial hard scattering produces a parton and an electroweak boson: the bosons do not experience quantum chromodynamic interactions and are largely unaffected by the QGP. At leading order, bosons are produced back to back with an associated parton having close to the same p_T , modulo secondary effects such as multiple scatterings of the initial partons or initial state radiation. As a result, the jets associated with the boson should have parent partons whose p_T before any energy loss occurs is well defined. In addition, at LHC energies, the electroweak-boson + jet production is dominated by quark jets for $p_T^{\text{jet}} > 30$ GeV/ c [25–27], therefore providing information specifically on quark energy loss.

The CMS Collaboration measured the azimuthal correlation and momentum imbalance of isolated-photon+jet pairs in pp and Pb-Pb collisions at nucleon-nucleon center-of-mass energies of $\sqrt{s_{\text{NN}}} = 2.76$ and 5.02 TeV [28,29] and of Z + jet pairs at $\sqrt{s_{\text{NN}}} = 5.02$ TeV [30]. In related studies, experiments at RHIC extracted jet fragmentation functions associated with photons without fully reconstructing the jets, but rather by studying direct-photon+hadron correlations [31,32]. This Letter presents the first measurement of the fragmentation function of jets that are fully reconstructed and associated with an isolated photon (i.e., one with no significant energy deposited around its location in the detector). This definition suppresses dijet events in which a high- p_T photon originates from one of the jets, either via collinear fragmentation of a parton (“fragmentation photons”) or via decays of neutral mesons

*Full author list given at the end of the Letter.

Published by the American Physical Society under the terms of the [Creative Commons Attribution 4.0 International license](https://creativecommons.org/licenses/by/4.0/). Further distribution of this work must maintain attribution to the author(s) and the published article’s title, journal citation, and DOI. Funded by SCOAP³.

(“decay photons”). The analysis uses Pb-Pb and pp data at $\sqrt{s_{\text{NN}}} = 5.02$ TeV collected in 2015 and corresponding to integrated luminosities of $404 \mu\text{b}^{-1}$ and 27.4pb^{-1} , respectively.

Photon-tagged fragmentation functions are presented as distributions of $\xi^{\text{jet}} = \ln [|\vec{p}^{\text{jet}}|^2 / (\vec{p}^{\text{trk}} \cdot \vec{p}^{\text{jet}})]$, where \vec{p}^{jet} and \vec{p}^{trk} are the 3-momenta of the jet and charged particle, respectively, and $\xi_T^{\text{jet}} = \ln [-|\vec{p}_T^{\text{jet}}|^2 / (\vec{p}_T^{\text{trk}} \cdot \vec{p}_T^{\text{jet}})]$, where \vec{p}_T^{jet} and \vec{p}_T^{trk} are the p_T with respect to the beam direction of the photon and charged particle, respectively. The ξ^{jet} variable gives the fragmentation pattern with respect to p_T of the reconstructed jet [33,34], and can be compared directly with results obtained using a dijet sample [18]. The ξ_T^{jet} variable is used to characterize the fragmentation pattern with respect to the p_T of the initial parton before any energy loss occurred. The \vec{p}_T^{jet} is used instead of \vec{p}^{jet} because the photon and parton from a hard scattering have the same $|p_T|$ at leading order, but not necessarily the same magnitude of longitudinal momentum.

The central feature of the CMS detector is a superconducting solenoid, providing a magnetic field of 3.8 T. Within the solenoid volume are a pixel and strip tracker, an electromagnetic calorimeter (ECAL), and a hadron calorimeter (HCAL). Hadron forward (HF) calorimeters extend the pseudorapidity coverage up to $|\eta| = 5.2$. In the case of Pb-Pb events, the HF signals are used to determine the degree of overlap (“centrality”) of the two colliding Pb nuclei [21] and the event-by-event azimuthal angle of maximum particle density (“event plane”) [35]. A more detailed description of the CMS detector can be found in Ref. [36].

The event samples are selected online with a dedicated photon trigger requiring one photon with $p_T^{\gamma} > 40$ GeV/ c [29], and are subjected to offline requirements to remove noncollision events [29,37]. For jets and photons, the reconstruction algorithms, analysis selections, and corrections for the energy scale and resolution are the same as in Ref. [29]. For the analysis of Pb-Pb collisions, the event centrality is defined as the fraction of the total inelastic hadronic cross section, starting at 0% for the most central collisions, and is evaluated as percentiles of the distribution of the energy deposited in the HF calorimeters [21]. Results are presented in four centrality intervals, ranging from a central 0%–10% (i.e., the 10% of the events having the largest overlap area of the two nuclei [38]), to a peripheral 50%–100% (the one closest to a pp -like environment) intervals.

The photon candidates are restricted to the barrel region of the ECAL, $|\eta^{\gamma}| < 1.44$, and are required to have $p_T^{\gamma} > 60$ GeV/ c . Electron contamination and anomalous signals caused by the interaction of heavily ionizing particles with the silicon avalanche photodiodes used for the ECAL readout are removed [39]. Background from ECAL showers induced by hadrons are rejected using the ratio of HCAL over ECAL energy inside a cone of radius

$\Delta R = \sqrt{(\Delta\eta)^2 + (\Delta\phi)^2} = 0.15$ around the photon candidate [39,40]. Background contributions from fragmentation and decay photons are rejected by imposing isolation requirements [29,39]. The dominant remaining background is ECAL showers initiated by isolated neutral mesons decaying into pairs of photons that are reconstructed as a single photon. Because the pattern of energy deposited in the ECAL (i.e., the “shower shape”) is wider in η for these decay photons, their contribution can be reduced by a factor of ~ 2 using an upper limit on the width of the η distribution [39].

The energy of the reconstructed photons is corrected to account for the effects of the material in front of the ECAL and for incomplete containment of the shower energy in the ECAL crystals [41]. An additional correction is applied in Pb-Pb collisions to account for the contribution of the underlying event (UE). The corrections are obtained from photon events simulated using the CUETP8M1 tune [42] of the PYTHIA 8.212 [43] Monte Carlo (MC) event generator. The effect of the Pb-Pb UE is modeled by embedding the PYTHIA output in events generated using HYDJET 1.9 [44]. The background simulation is tuned to reproduce the observed charged-particle multiplicity and p_T spectrum in Pb-Pb data. The size of the resulting energy correction for isolated photons varies from 0% to 10%, depending on p_T^{γ} and the centrality of the collision.

The particle-flow algorithm [45] is used for the jet reconstruction with the anti- k_T algorithm provided in the FASTJET framework [46,47] with a distance parameter $R = 0.3$. In order to subtract the UE background in Pb-Pb collisions, an iterative algorithm [48] is employed [21,28,49]. In pp collisions, where the UE level is negligible, jets are reconstructed without UE subtraction (for a jet with $p_T = 30$ GeV/ c , the UE contribution is at most 1%). The jet energy corrections are derived from simulation, separately for pp and Pb-Pb, and are confirmed via energy-balance methods in pp data [50]. Jets with $|\eta^{\text{jet}}| < 1.6$ and corrected $p_T^{\text{jet}} > 30$ GeV/ c are selected. In order to compare the Pb-Pb and pp results, the jet energy and ϕ^{jet} in pp events are smeared to match the corresponding resolutions in each of the Pb-Pb centrality intervals. The parametrization of the energy smearing function is given in Ref. [29]. To match the 0%–10% Pb-Pb data, the energy resolution of pp jets with $p_T^{\text{jet}} = 30(90)$ GeV/ c changes from 18% (12%) to 35% (17%). The change in angular resolution is negligible ($< 2.2\%$).

In each event, photon + jet pairs are formed by associating the highest- p_T^{γ} isolated photon candidate with all jets that pass the jet selection criteria. An azimuthal separation of $\Delta\phi_{j\gamma} = |\phi^{\text{jet}} - \phi^{\gamma}| > 7\pi/8$ is applied to the photon + jet pairs to suppress contributions from background jets (not from the same hard scattering as the photon) and photon + multijet events (from an early splitting of the original parton). The tracks used in the measurement of the

fragmentation function have $p_T^{\text{trk}} > 1 \text{ GeV}/c$ and are required to fall within a cone of radius $\Delta R = 0.3$ around the jet direction. These selection criteria, as well as the corrections for tracking efficiency, detector acceptance, and misreconstruction rate, are the same as in Ref. [37].

The selected charged-particle tracks (N^{trk}) are used in conjunction with the selected photon + jet pairs to determine the fragmentation functions, $(1/N^{\text{jet}})(dN^{\text{trk}}/d\xi^{\text{jet}})$ and $(1/N^{\text{jet}})(dN^{\text{trk}}/d\xi_T^{\text{jet}})$, where N^{jet} represents the total number of photon + jet pairs. To isolate the contribution of photons, jets, and charged particles that are produced in the same hard scattering in Pb-Pb collisions, several combinatorial backgrounds are subtracted: tracks from the UE that fall within the cone around the selected jet, misidentified jets resulting from UE fluctuations, and jets not produced in the same hard parton-parton scatterings as the photon. The shape and magnitude of these contributions are estimated from data with an event mixing procedure, in which either the isolated photon or the jet is combined with jets and tracks found in events chosen randomly from a minimum-bias (MB) Pb-Pb data set with similar event characteristics (centrality, interaction vertex position, and event plane angle). The background contribution from UE tracks is estimated by correlating each selected jet with tracks from MB events. The backgrounds from jets produced by UE fluctuations or a different parton-parton scattering are estimated by correlating each selected photon with jets from randomly selected MB events as in Refs. [28,29]. The normalizations of these combinatorial background fragmentation functions are given by the number of MB events used. Simulations predict that the average UE particle density is slightly different between a MB event and an event containing a hard scattering, even when the two have the same collision centrality. Therefore, the normalized background distributions are further scaled with a residual factor to account for this effect. The final correction accounts for the photon purity, defined to be the fraction of nondecay photons within the collection of isolated photon candidates that pass the shower shape requirement. This fraction is extracted from the data using a template fit to the shower shape distribution, and is $\sim 65\%$ (85%) in $0\%–10\%$ ($0\%–50\%$) PbPb collisions [28,29]. The shape of the fragmentation functions from decay photons is estimated by repeating the analysis selecting photons with wider shower shapes.

Several sources of systematic uncertainty are considered: photon purity, energy scale, isolation, electron contamination, jet energy scale and resolution, tracking efficiency, and UE background. The total uncertainty is the sum in quadrature of the individual uncertainties. The quoted systematic uncertainties are an average over all ξ^{jet} and ξ_T^{jet} bins and, in the case of the Pb-Pb results, are quoted only for events with $0\%–10\%$ centrality. To evaluate the systematic uncertainties related to the isolated photons, the same procedures as in Ref. [29] are applied. The uncertainty in the

photon purity estimation is evaluated by varying the components of the shower shape template [28]. The maximum variations with respect to the nominal case are propagated as systematic uncertainties, amounting to 2.8 (5.4)% for the Pb-Pb events, and 0.4 (0.4)% for the pp results, for ξ^{jet} (ξ_T^{jet}). In the following, the uncertainties will continue to be quoted for central Pb-Pb first, then for pp . The total systematic uncertainties resulting from the experimental criteria for an isolated photon are 1.7 (1.1)% and 0.9 (0.7)% for ξ^{jet} (ξ_T^{jet}). The residual data-to-simulation photon energy scale difference after applying the photon energy corrections is also quoted as a systematic uncertainty of 1.2 (1.2)% and $< 0.1\%$ for ξ^{jet} (ξ_T^{jet}). An uncertainty for the level of electron contamination is evaluated by repeating the analysis without applying the electron rejection criteria, and scaling down the difference in the ξ observables to the remaining electron level of contamination after applying the electron rejection, giving 0.6 (0.5)% and < 0.1 (0.1)% for ξ^{jet} (ξ_T^{jet}). The efficiency for selecting photons has been extracted from MC calculations as a function of photon p_T . An uncertainty is assigned by comparing the results to the ones obtained with a correction derived after loosening the selection criteria, giving 0.1 (0.5)% and < 0.1 (< 0.1)% for ξ^{jet} (ξ_T^{jet}). The uncertainty related to the jet energy scale [29] amounts to 7.3 (6.5)% and 2.4 (0.6)% for ξ^{jet} (ξ_T^{jet}), while the energy resolution [29] gives uncertainties of 2.8 (1.7)% and 0.7 (0.5)%. A systematic uncertainty is assigned to account for long-range η correlations [23] that contribute to the UE. It is estimated by constructing the observables using tracks lying within the same azimuthal angle as the jet, but separated by a large pseudorapidity interval, $1.5 < \Delta\eta < 2.4$. The uncertainty is found to be 4.1 (3.3)% and 1.7 (1.5)% for ξ^{jet} (ξ_T^{jet}). The uncertainty related to the tracking inefficiency is estimated as the difference in the track reconstruction efficiency between data and simulation [37]. It is 5 (4)% for Pb-Pb (pp) data, for both ξ^{jet} and ξ_T^{jet} , and is constant as a function of the track p_T and event centrality.

For the Pb-Pb results only, two additional sources of systematic uncertainties are considered. One accounts for possible inaccuracies in the background subtraction by combining two independent components. First, the effect of the background subtraction method is estimated using an alternative procedure (the so-called η -reflection method [18]), which has different sensitivities to various background sources. Second, results are compared to the ones where background distributions are not scaled for the UE particle density difference seen when comparing simulated MB events with those containing a hard scattering. The combined difference of 3.6 (3.5)% for ξ^{jet} (ξ_T^{jet}) is assigned as the uncertainty. The second uncertainty accounts for differences in the jet energy response due to ξ^{jet} and ξ_T^{jet} variances in the jet fragmentation pattern, as studied in simulation [29]. The observed differences of 11% for $\xi^{\text{jet}} < 1$ and 4.3 (7.0)% for $\xi^{\text{jet}}(\xi_T^{\text{jet}}) > 2.5$ are propagated

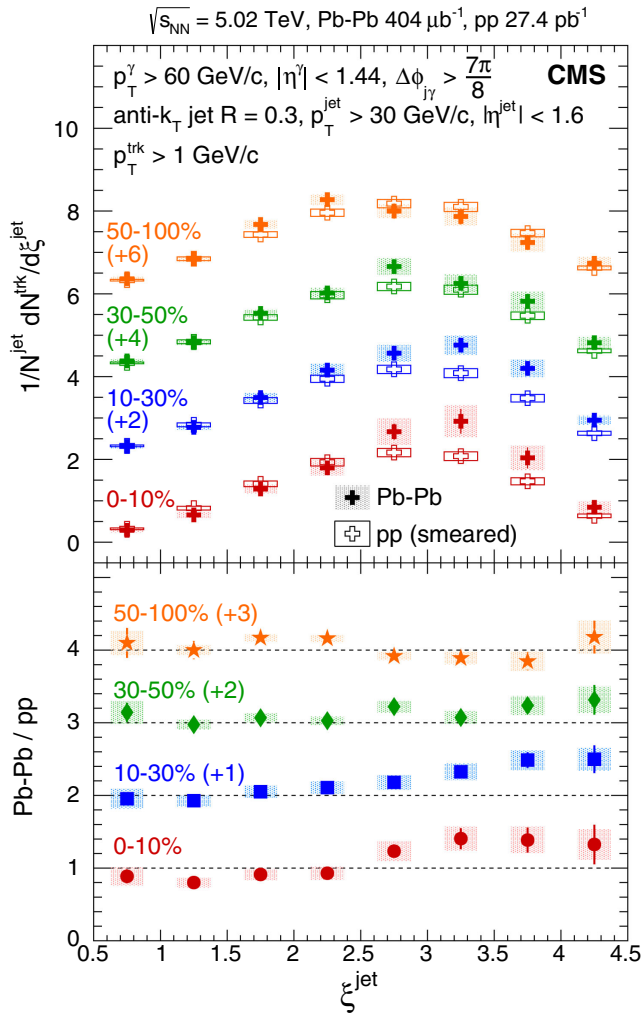


FIG. 1. Top: centrality dependence of the ξ^{jet} distribution for jets associated with an isolated photon for Pb-Pb (full crosses) and pp (open crosses) collisions. The pp results are smeared for each Pb-Pb centrality bin, and data for each centrality bin are shifted vertically as indicated. Bottom: ratios of the Pb-Pb over smeared pp distributions. The vertical bars through the points represent statistical uncertainties, while the colored boxes indicate systematic uncertainties.

as uncertainties in the corresponding ξ^{jet} and ξ_T^{jet} regions for the Pb-Pb results, while there are no significant differences in other ξ^{jet} and ξ_T^{jet} bins.

Figure 1 shows the photon-tagged fragmentation functions as a function of ξ^{jet} for both Pb-Pb and pp collisions, together with their ratio of the Pb-Pb to pp results. The ξ^{jet} distributions in Pb-Pb collisions represent the fragmentation pattern of jets that may have lost energy through interactions with the medium, while those for pp stand for unquenched jets. Because of this possibility of quenching, the collections of reconstructed jets in Pb-Pb and pp collisions do not necessarily have the same p_T^{jet} spectrum, even though the samples are selected based on photon energy. The ξ^{jet} distributions for 50%–100% centrality

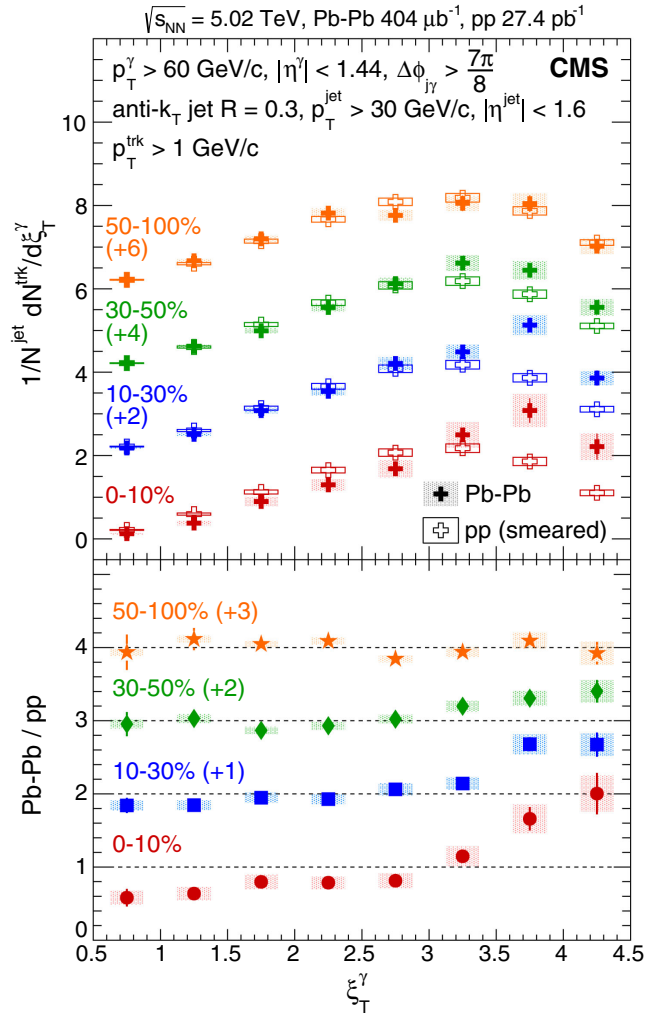


FIG. 2. Top: centrality dependence of the ξ_T^{jet} distribution for jets associated with an isolated photon for Pb-Pb (full crosses) and pp (open crosses) collisions. The pp results are smeared for each Pb-Pb centrality bin, and data for each centrality bin are shifted vertically as indicated. Bottom: ratios of the Pb-Pb over smeared pp distributions. The vertical bars through the points represent statistical uncertainties, while the colored boxes indicate systematic uncertainties.

Pb-Pb collisions are consistent with those in pp collisions. In more central collisions, an enhancement of the fragmentation function in Pb-Pb collisions with respect to the reference pp data is observed for $\xi^{\text{jet}} > 2.5$ (corresponding to $p_T^{\text{trk}} \lesssim 2.5$ GeV/ c for $p_T^{\text{jet}} = 30$ GeV/ c and $\Delta R = 0$ between the track and the jet), indicating that there is a small excess of soft particles near the jet. Additionally, a slight suppression of the fragmentation function in the region $0.5 < \xi^{\text{jet}} < 2.5$ (corresponding to $18 \gtrsim p_T^{\text{trk}} \gtrsim 2.5$ GeV/ c for $p_T^{\text{jet}} = 30$ GeV/ c and $\Delta R = 0$) is also observed in the most central Pb-Pb collisions.

Figure 2 shows the photon-tagged fragmentation functions as a function of ξ_T^{jet} for Pb-Pb and pp collisions, as well as their ratio. As for ξ^{jet} , the ξ_T^{jet} distributions for

peripheral Pb-Pb events are consistent with those in pp data. In more central collisions, an enhancement is observed in the Pb-Pb data relative to pp data in the $\xi_T^{\gamma} > 3$ region (corresponding to $p_T^{\text{trk}} \lesssim 3$ GeV/ c for $p_T^{\gamma} = 60$ GeV/ c and $\Delta\phi = \pi$ between the track and the photon). The magnitude of this enhancement increases as the Pb-Pb collisions become more central, and is more significant than the enhancement observed in the ξ^{jet} distributions. The differences between the pp and Pb-Pb distributions are quantified by comparing the two distributions using a χ^2 test. The p values from the test are 10^{-3} and 10^{-20} for the ξ^{jet} and ξ_T^{γ} distributions, respectively. Similarly, the ξ^{jet} distribution was compared to that for ξ_T^{γ} within the same system. The p values from the test are 10^{-3} and 10^{-10} for the Pb-Pb and pp results, respectively. A suppression of the ξ_T^{γ} distribution for the most central Pb-Pb collisions is also observed for $0.5 < \xi_T^{\gamma} < 3$ (corresponding to $36 \gtrsim p_T^{\text{trk}} \gtrsim 3$ GeV/ c for $p_T^{\gamma} = 60$ GeV/ c and $\Delta\phi = \pi$). This pattern of suppression and enhancement is direct evidence for energy loss by high- p_T partons as they traverse the high-density medium created in heavy ion collisions [51,52].

The enhancement at large ξ^{jet} and ξ_T^{γ} , together with the suppression at lower values, indicates that the showers of partons that emerge from the medium contain more lower-energy particles in Pb-Pb collisions. These particles can originate directly from high-energy partons that lose energy, as well as from the medium response, the recoil of the medium as the parton traverses through [34,53,54]. The enhancements and suppressions of the fragmentation patterns measured using a photon to estimate the initial parton energy (ξ_T^{γ}) are observed to be more pronounced than the ones measured using detector level jet energy (ξ^{jet}). Qualitatively, this is not surprising. Because of effects such as out-of-cone radiation not being captured in the anti- k_T $R = 0.3$ jet area, a shift of the distributions to lower values for ξ^{jet} compared to ξ_T^{γ} is observed even in the pp results. In Pb-Pb collisions, an additional shift happens when the jet is quenched: the jet momentum becomes lower than that of the parton, resulting in a shift to lower ξ^{jet} . As a result, the modifications in the ratio Pb-Pb/ pp are weakened by quenching in the ξ^{jet} case. This analysis, using events selected with a photon trigger which ensures that the initial parton p_T spectra are the same for pp and Pb-Pb, will allow testing the theoretical modeling of both the parton shower modification in the medium and the medium response to the passage of that parton.

In summary, the fragmentation functions of jets associated with isolated photons are measured for the first time in pp and Pb-Pb data collected at $\sqrt{s_{\text{NN}}} = 5.02$ TeV by CMS. Fragmentation patterns as functions of $\xi^{\text{jet}} = \ln[|\vec{p}^{\text{jet}}|^2/(\vec{p}^{\text{trk}} \cdot \vec{p}^{\text{jet}})]$ and $\xi_T^{\gamma} = \ln[-|\vec{p}_T^{\gamma}|^2/(\vec{p}_T^{\text{trk}} \cdot \vec{p}_T^{\gamma})]$ are constructed using charged particles with $p_T^{\text{trk}} > 1$ GeV/ c , for jets with $p_T^{\text{jet}} > 30$ GeV/ c tagged by an isolated photon with $p_T^{\gamma} > 60$ GeV/ c . When compared to the pp results,

the ξ^{jet} and ξ_T^{γ} distributions in central Pb-Pb collisions show an excess of low- p_T particles and a depletion of high- p_T particles inside the jet. This observation is more apparent in the ξ_T^{γ} distributions, where the photon-based selection allows for tagging the properties of the initial parton before quenching occurs. This measurement shows for the first time the in-medium parton shower modifications for events with well-defined initial parton kinematics, and constitutes a new well-controlled reference for testing theoretical models of the parton's passage through the QGP.

We congratulate our colleagues in the CERN accelerator departments for the excellent performance of the LHC and thank the technical and administrative staffs at CERN and at other CMS institutes for their contributions to the success of the CMS effort. In addition, we gratefully acknowledge the computing centers and personnel of the Worldwide LHC Computing Grid for delivering so effectively the computing infrastructure essential to our analyses. Finally, we acknowledge the enduring support for the construction and operation of the LHC and the CMS detector provided by the following funding agencies: BMFWF and FWF (Austria); FNRS and FWO (Belgium); CNPq, CAPES, FAPERJ, and FAPESP (Brazil); MES (Bulgaria); CERN; CAS, MoST, and NSFC (China); COLCIENCIAS (Colombia); MSES and CSF (Croatia); RPF (Cyprus); SENESCYT (Ecuador); MoER, ERC IUT, and ERDF (Estonia); Academy of Finland, MEC, and HIP (Finland); CEA and CNRS/IN2P3 (France); BMBF, DFG, and HGF (Germany); GSRT (Greece); OTKA and NIH (Hungary); DAE and DST (India); IPM (Iran); SFI (Ireland); INFN (Italy); MSIP and NRF (Republic of Korea); LAS (Lithuania); MOE and UM (Malaysia); BUAP, CINVESTAV, CONACYT, LNS, SEP, and UASLP-FAI (Mexico); MBIE (New Zealand); PAEC (Pakistan); MSHE and NSC (Poland); FCT (Portugal); JINR (Dubna); MON, Federal Agency of Atomic Energy of the Russian Federation, RosAtom, RAS, RFBR and RAEP (Russia); MESTD (Serbia); SEIDI, CPAN, PCTI and FEDER (Spain); Swiss Funding Agencies (Switzerland); MST (Taipei); ThEPCenter, IPST, STAR, and NSTDA (Thailand); TUBITAK and TAEK (Turkey); NASU and SFFR (Ukraine); STFC (United Kingdom); DOE and NSF (USA).

-
- [1] F. Karsch, The phase transition to the quark gluon plasma: Recent results from lattice calculations, *Nucl. Phys.* **A590**, 367 (1995).
 - [2] J. D. Bjorken, Highly relativistic nucleus-nucleus collisions: The central rapidity region, *Phys. Rev. D* **27**, 140 (1983).
 - [3] D. A. Appel, Jets as a probe of quark-gluon plasmas, *Phys. Rev. D* **33**, 717 (1986).
 - [4] J. P. Blaizot and L. D. McLerran, Jets in expanding quark-gluon plasmas, *Phys. Rev. D* **34**, 2739 (1986).
 - [5] M. Gyulassy and M. Plümer, Jet quenching in dense matter, *Phys. Lett. B* **243**, 432 (1990).

- [6] X.-N. Wang and M. Gyulassy, Gluon Shadowing and Jet Quenching in $A + A$ Collisions at $\sqrt{s} = 200A$ GeV, *Phys. Rev. Lett.* **68**, 1480 (1992).
- [7] R. Baier, Y. L. Dokshitzer, A. H. Mueller, S. Peigne, and D. Schiff, Radiative energy loss and p_{\perp} -broadening of high energy partons in nuclei, *Nucl. Phys.* **B484**, 265 (1997).
- [8] B. G. Zakharov, Radiative energy loss of high-energy quarks in finite-size nuclear matter and quark-gluon plasma, *JETP Lett.* **65**, 615 (1997).
- [9] M. Gyulassy, P. Levai, and I. Vitev, Reaction operator approach to nonAbelian energy loss, *Nucl. Phys.* **B594**, 371 (2001).
- [10] M. Djordjevic and M. Gyulassy, Heavy quark radiative energy loss in QCD matter, *Nucl. Phys.* **A733**, 265 (2004).
- [11] G. Ovanessian and I. Vitev, An effective theory for jet propagation in dense QCD matter: Jet broadening and medium-induced bremsstrahlung, *J. High Energy Phys.* **06** (2011) 080.
- [12] X.-N. Wang and X.-f. Guo, Multiple parton scattering in nuclei: Parton energy loss, *Nucl. Phys.* **A696**, 788 (2001).
- [13] P. B. Arnold, G. D. Moore, and L. G. Yaffe, Photon and gluon emission in relativistic plasmas, *J. High Energy Phys.* **06** (2002) 030.
- [14] K. M. Burke *et al.* (JET Collaboration), Extracting the jet transport coefficient from jet quenching in high-energy heavy-ion collisions, *Phys. Rev. C* **90**, 014909 (2014).
- [15] ATLAS Collaboration, Measurements of the Nuclear Modification Factor for Jets in Pb + Pb Collisions at $\sqrt{s_{NN}} = 2.76$ TeV with the ATLAS Detector, *Phys. Rev. Lett.* **114**, 072302 (2015).
- [16] ALICE Collaboration, Measurement of jet suppression in central Pb-Pb collisions at $\sqrt{s_{NN}} = 2.76$ TeV, *Phys. Lett. B* **746**, 1 (2015).
- [17] CMS Collaboration, Measurement of inclusive jet cross sections in pp and PbPb collisions at $\sqrt{s_{NN}} = 2.76$ TeV, *Phys. Rev. C* **96**, 015202 (2017).
- [18] CMS Collaboration, Measurement of jet fragmentation in PbPb and pp collisions at $\sqrt{s_{NN}} = 2.76$ TeV, *Phys. Rev. C* **90**, 024908 (2014).
- [19] ATLAS Collaboration, Measurement of jet fragmentation in Pb + Pb and pp collisions at $\sqrt{s_{NN}} = 2.76$ TeV with the ATLAS detector at the LHC, *Eur. Phys. J. C* **77**, 379 (2017).
- [20] ATLAS Collaboration, Observation of a Centrality-Dependent Dijet Asymmetry in Lead-Lead Collisions at $\sqrt{s_{NN}} = 2.76$ TeV with the ATLAS Detector at the LHC, *Phys. Rev. Lett.* **105**, 252303 (2010).
- [21] CMS Collaboration, Observation and studies of jet quenching in PbPb collisions at $\sqrt{s_{NN}} = 2.76$ TeV, *Phys. Rev. C* **84**, 024906 (2011).
- [22] CMS Collaboration, Measurement of transverse momentum relative to dijet systems in PbPb and pp collisions at $\sqrt{s_{NN}} = 2.76$ TeV, *J. High Energy Phys.* **01** (2016) 006.
- [23] CMS Collaboration, Decomposing transverse momentum balance contributions for quenched jets in PbPb collisions at $\sqrt{s_{NN}} = 2.76$ TeV, *J. High Energy Phys.* **11** (2016) 055.
- [24] CMS Collaboration, Modification of jet shapes in PbPb collisions at $\sqrt{s_{NN}} = 2.76$ TeV, *Phys. Lett. B* **730**, 243 (2014).
- [25] R. B. Neufeld, I. Vitev, and B. W. Zhang, Physics of Z^0/γ^* -tagged jets at energies available at the CERN Large Hadron Collider, *Phys. Rev. C* **83**, 034902 (2011).
- [26] Z.-Bo Kang, I. Vitev, and H. Xing, Vector-boson-tagged jet production in heavy ion collisions at energies available at the CERN Large Hadron Collider, *Phys. Rev. C* **96**, 014912 (2017).
- [27] W. Dai and I. Vitev, and B.-W. Zhang, Momentum Imbalance of Isolated Photon-Tagged Jet Production at RHIC and LHC, *Phys. Rev. Lett.* **110**, 142001 (2013).
- [28] CMS Collaboration, Studies of jet quenching using isolated-photon+jet correlations in PbPb and pp collisions at $\sqrt{s_{NN}} = 2.76$ TeV, *Phys. Lett. B* **718**, 773 (2013).
- [29] CMS Collaboration, Study of jet quenching with isolated-photon + jet correlations in PbPb and pp collisions at $\sqrt{s_{NN}} = 5.02$ TeV, *Phys. Lett. B* **785**, 14 (2018).
- [30] CMS Collaboration, Study of Jet Quenching with $Z + \text{jet}$ Correlations in Pb-Pb and pp Collisions at $\sqrt{s_{NN}} = 5.02$ TeV, *Phys. Rev. Lett.* **119**, 082301 (2017).
- [31] A. Adare *et al.* (PHENIX Collaboration), Medium Modification of Jet Fragmentation in Au+Au Collisions at $\sqrt{s_{NN}} = 200$ GeV Measured in Direct Photon-Hadron Correlations, *Phys. Rev. Lett.* **111**, 032301 (2013).
- [32] L. Adamczyk *et al.* (STAR Collaboration), Jet-like correlations with direct-photon and neutral-pion triggers at $\sqrt{s_{NN}} = 200$ GeV, *Phys. Lett. B* **760**, 689 (2016).
- [33] F. Arleo, P. Aurenche, Z. Belghobsi, and J.-P. Guillet, Photon tagged correlations in heavy ion collisions, *J. High Energy Phys.* **11** (2004) 009.
- [34] J. Casalderrey-Solana, D. C. Gulhan, J. G. Milhano, D. Pablos, and K. Rajagopal, Predictions for boson-jet observables and fragmentation function ratios from a hybrid strong/weak coupling model for jet quenching, *J. High Energy Phys.* **03** (2016) 053.
- [35] CMS Collaboration, Azimuthal Anisotropy of Charged Particles at High Transverse Momenta in PbPb Collisions at $\sqrt{s_{NN}} = 2.76$ TeV, *Phys. Rev. Lett.* **109**, 022301 (2012).
- [36] CMS Collaboration, The CMS experiment at the CERN LHC, *J. Instrum.* **3**, S08004 (2008).
- [37] CMS Collaboration, Charged-particle nuclear modification factors in PbPb and pPb collisions at $\sqrt{s_{NN}} = 5.02$ TeV, *J. High Energy Phys.* **04** (2017) 039.
- [38] M. L. Miller, K. Reygers, S. J. Sanders, and P. Steinberg, Glauber modeling in high energy nuclear collisions, *Annu. Rev. Nucl. Part. Sci.* **57**, 205 (2007).
- [39] CMS Collaboration, Measurement of isolated photon production in pp and PbPb collisions at $\sqrt{s_{NN}} = 2.76$ TeV, *Phys. Lett. B* **710**, 256 (2012).
- [40] CMS Collaboration, Measurement of the Isolated Prompt Photon Production Cross Section in pp Collisions at $\sqrt{s} = 7$ TeV, *Phys. Rev. Lett.* **106**, 082001 (2011).
- [41] CMS Collaboration, Performance of photon reconstruction and identification with the CMS detector in proton-proton collisions at $\sqrt{s} = 8$ TeV, *J. Instrum.* **10**, P08010 (2015).
- [42] CMS Collaboration, Event generator tunes obtained from underlying event and multiparton scattering measurements, *Eur. Phys. J. C* **76**, 155 (2016).

- [43] T. Sjöstrand, S. Ask, J. R. Christiansen, R. Corke, N. Desai, P. Ilten, S. Mrenna, S. Prestel, C. O. Rasmussen, and P. Z. Skands, An introduction to PYTHIA 8.2, *Comput. Phys. Commun.* **191**, 159 (2015).
- [44] I. P. Lokhtin and A. M. Snigirev, A model of jet quenching in ultrarelativistic heavy ion collisions and high- p_T hadron spectra at RHIC, *Eur. Phys. J. C* **45**, 211 (2006).
- [45] CMS Collaboration, Particle-flow reconstruction and global event description with the CMS detector, *J. Instrum.* **12**, P10003 (2017).
- [46] M. Cacciari, G. P. Salam, and G. Soyez, The anti- k_t jet clustering algorithm, *J. High Energy Phys.* **04** (2008) 063.
- [47] M. Cacciari, G. P. Salam, and G. Soyez, FastJet user manual, *Eur. Phys. J. C* **72**, 1896 (2012).
- [48] O. Kodolova, I. Vardanian, A. Nikitenko, and A. Oulianov, The performance of the jet identification and reconstruction in heavy ions collisions with CMS detector, *Eur. Phys. J. C* **50**, 117 (2007).
- [49] CMS Collaboration, Jet momentum dependence of jet quenching in PbPb collisions at $\sqrt{s_{NN}} = 2.76$ TeV, *Phys. Lett. B* **712**, 176 (2012).
- [50] CMS Collaboration, Jet energy scale and resolution in the CMS experiment in pp collisions at 8 TeV, *J. Instrum.* **12**, P02014 (2017).
- [51] X.-N. Wang, Z. Huang, and I. Sarcevic, Jet Quenching in the Opposite Direction of a Tagged Photon in High-Energy Heavy Ion Collisions, *Phys. Rev. Lett.* **77**, 231 (1996).
- [52] X.-N. Wang and Z. Huang, Medium-induced parton energy loss in γ + jet events of high-energy heavy-ion collisions, *Phys. Rev. C* **55**, 3047 (1997).
- [53] R. K. Elayavalli and K. C. Zapp, Medium response in JEWEL and its impact on jet shape observables in heavy ion collisions, *J. High Energy Phys.* **07** (2017) 141.
- [54] X.-N. Wang and Y. Zhu, Medium Modification of γ -Jets in High-Energy Heavy-Ion Collisions, *Phys. Rev. Lett.* **111**, 062301 (2013).

A. M. Sirunyan,¹ A. Tumasyan,¹ W. Adam,² F. Ambrogio,² E. Asilar,² T. Bergauer,² J. Brandstetter,² E. Brondolin,² M. Dragicevic,² J. Erö,² A. Escalante Del Valle,² M. Flechl,² M. Friedl,² R. Frühwirth,^{2,b} V. M. Ghete,² J. Grossmann,² J. Hrubec,² M. Jeitler,^{2,b} A. König,² N. Krammer,² I. Krätschmer,² D. Liko,² T. Madlener,² I. Mikulec,² E. Pree,² N. Rad,² H. Rohringer,² J. Schieck,^{2,b} R. Schöfbeck,² M. Spanring,² D. Spitzbart,² A. Taurok,² W. Waltenberger,² J. Wittmann,² C.-E. Wulz,^{2,b} M. Zarucki,² V. Chekhovsky,³ V. Mossolov,³ J. Suarez Gonzalez,³ E. A. De Wolf,⁴ D. Di Croce,⁴ X. Janssen,⁴ J. Lauwers,⁴ M. Van De Klundert,⁴ H. Van Haevermaet,⁴ P. Van Mechelen,⁴ N. Van Remortel,⁴ S. Abu Zeid,⁵ F. Blekman,⁵ J. D'Hondt,⁵ I. De Bruyn,⁵ J. De Clercq,⁵ K. Deroover,⁵ G. Flouris,⁵ D. Lontkovskiy,⁵ S. Lowette,⁵ I. Marchesini,⁵ S. Moortgat,⁵ L. Moreels,⁵ Q. Python,⁵ K. Skovpen,⁵ S. Tavernier,⁵ W. Van Doninck,⁵ P. Van Mulders,⁵ I. Van Parijs,⁵ D. Beghin,⁶ B. Bilin,⁶ H. Brun,⁶ B. Clerbaux,⁶ G. De Lentdecker,⁶ H. Delannoy,⁶ B. Dorney,⁶ G. Fasanella,⁶ L. Favart,⁶ R. Goldouzian,⁶ A. Grebenyuk,⁶ A. K. Kalsi,⁶ T. Lenzi,⁶ J. Luetic,⁶ T. Maerschalk,⁶ A. Marinov,⁶ T. Seva,⁶ E. Starling,⁶ C. Vander Velde,⁶ P. Vanlaer,⁶ D. Vannerom,⁶ R. Yonamine,⁶ F. Zenoni,⁶ T. Cornelis,⁷ D. Dobur,⁷ A. Fagot,⁷ M. Gul,⁷ I. Khvastunov,^{7,c} D. Poyraz,⁷ C. Roskas,⁷ S. Salva,⁷ D. Trocino,⁷ M. Tytgat,⁷ W. Verbeke,⁷ M. Vit,⁷ N. Zaganidis,⁷ H. Bakhshiansohi,⁸ O. Bondu,⁸ S. Brochet,⁸ G. Bruno,⁸ C. Caputo,⁸ A. Caudron,⁸ P. David,⁸ S. De Visscher,⁸ C. Delaere,⁸ M. Delcourt,⁸ B. Francois,⁸ A. Giammanco,⁸ M. Komm,⁸ G. Krintiras,⁸ V. Lemaître,⁸ A. Magitteri,⁸ A. Mertens,⁸ M. Musich,⁸ K. Piotrkowski,⁸ L. Quertenmont,⁸ A. Saggio,⁸ M. Vidal Marono,⁸ S. Wertz,⁸ J. Zobec,⁸ W. L. Aldá Júnior,⁹ F. L. Alves,⁹ G. A. Alves,⁹ L. Brito,⁹ G. Correia Silva,⁹ C. Hensel,⁹ A. Moraes,⁹ M. E. Pol,⁹ P. Rebello Teles,⁹ E. Belchior Batista Das Chagas,¹⁰ W. Carvalho,¹⁰ J. Chinellato,^{10,d} E. Coelho,¹⁰ E. M. Da Costa,¹⁰ G. G. Da Silveira,^{10,e} D. De Jesus Damiao,¹⁰ S. Fonseca De Souza,¹⁰ L. M. Huertas Guativa,¹⁰ H. Malbouisson,¹⁰ M. Melo De Almeida,¹⁰ C. Mora Herrera,¹⁰ L. Mundim,¹⁰ H. Nogima,¹⁰ L. J. Sanchez Rosas,¹⁰ A. Santoro,¹⁰ A. Sznajder,¹⁰ M. Thiel,¹⁰ E. J. Tonelli Manganote,^{10,d} F. Torres Da Silva De Araujo,¹⁰ A. Vilela Pereira,¹⁰ S. Ahuja,^{11a} C. A. Bernardes,^{11a} T. R. Fernandez Perez Tomei,^{11a} E. M. Gregores,^{11a,11b} P. G. Mercadante,^{11a,11b} S. F. Novaes,^{11a} Sandra S. Padula,^{11a} D. Romero Abad,^{11a,11b} J. C. Ruiz Vargas,^{11a} A. Aleksandrov,¹² R. Hadjiiska,¹² P. Iaydjiev,¹² M. Misheva,¹² M. Rodozov,¹² M. Shopova,¹² G. Sultanov,¹² A. Dimitrov,¹³ L. Litov,¹³ B. Pavlov,¹³ P. Petkov,¹³ W. Fang,^{14,f} X. Gao,^{14,f} L. Yuan,¹⁴ M. Ahmad,¹⁵ J. G. Bian,¹⁵ G. M. Chen,¹⁵ H. S. Chen,¹⁵ M. Chen,¹⁵ Y. Chen,¹⁵ C. H. Jiang,¹⁵ D. Leggat,¹⁵ H. Liao,¹⁵ Z. Liu,¹⁵ F. Romeo,¹⁵ S. M. Shaheen,¹⁵ A. Spiezia,¹⁵ J. Tao,¹⁵ C. Wang,¹⁵ Z. Wang,¹⁵ E. Yazgan,¹⁵ H. Zhang,¹⁵ J. Zhao,¹⁵ Y. Ban,¹⁶ G. Chen,¹⁶ J. Li,¹⁶ Q. Li,¹⁶ S. Liu,¹⁶ Y. Mao,¹⁶ S. J. Qian,¹⁶ D. Wang,¹⁶ Z. Xu,¹⁶ F. Zhang,^{16,f} Y. Wang,¹⁷ C. Avila,¹⁸ A. Cabrera,¹⁸ C. A. Carrillo Montoya,¹⁸ L. F. Chaparro Sierra,¹⁸ C. Florez,¹⁸ C. F. González Hernández,¹⁸ J. D. Ruiz Alvarez,¹⁸ M. A. Segura Delgado,¹⁸ B. Courbon,¹⁹ N. Godinovic,¹⁹ D. Lelas,¹⁹ I. Puljak,¹⁹ P. M. Ribeiro Cipriano,¹⁹ T. Sculac,¹⁹ Z. Antunovic,²⁰ M. Kovac,²⁰ V. Brigljevic,²¹ D. Ferencek,²¹ K. Kadija,²¹ B. Mesic,²¹ A. Starodumov,^{21,g} T. Susa,²¹ M. W. Ather,²² A. Attikis,²² G. Mavromanolakis,²² J. Mousa,²² C. Nicolaou,²² F. Ptochos,²² P. A. Razis,²² H. Rykaczewski,²² M. Finger,^{23,h} M. Finger Jr.,^{23,h} E. Carrera Jarrin,²⁴ E. El-khateeb,^{25,i} A. Ellithi Kamel,^{25,j}

C. Tully,¹⁶⁵ S. Malik,¹⁶⁶ S. Norberg,¹⁶⁶ A. Barker,¹⁶⁷ V. E. Barnes,¹⁶⁷ S. Das,¹⁶⁷ S. Folgueras,¹⁶⁷ L. Gutay,¹⁶⁷ M. Jones,¹⁶⁷
 A. W. Jung,¹⁶⁷ A. Khatiwada,¹⁶⁷ D. H. Miller,¹⁶⁷ N. Neumeister,¹⁶⁷ C. C. Peng,¹⁶⁷ H. Qiu,¹⁶⁷ J. F. Schulte,¹⁶⁷ J. Sun,¹⁶⁷
 F. Wang,¹⁶⁷ R. Xiao,¹⁶⁷ W. Xie,¹⁶⁷ T. Cheng,¹⁶⁸ N. Parashar,¹⁶⁸ J. Stupak,¹⁶⁸ Z. Chen,¹⁶⁹ K. M. Ecklund,¹⁶⁹ S. Freed,¹⁶⁹
 F. J. M. Geurts,¹⁶⁹ M. Guilbaud,¹⁶⁹ M. Kilpatrick,¹⁶⁹ W. Li,¹⁶⁹ B. Michlin,¹⁶⁹ B. P. Padley,¹⁶⁹ J. Roberts,¹⁶⁹ J. Rorie,¹⁶⁹
 W. Shi,¹⁶⁹ Z. Tu,¹⁶⁹ J. Zabel,¹⁶⁹ A. Zhang,¹⁶⁹ A. Bodek,¹⁷⁰ P. de Barbaro,¹⁷⁰ R. Demina,¹⁷⁰ Y. t. Duh,¹⁷⁰ T. Ferbel,¹⁷⁰
 M. Galanti,¹⁷⁰ A. Garcia-Bellido,¹⁷⁰ J. Han,¹⁷⁰ O. Hindrichs,¹⁷⁰ A. Khukhunaishvili,¹⁷⁰ K. H. Lo,¹⁷⁰ P. Tan,¹⁷⁰ M. Verzetti,¹⁷⁰
 R. Ciesielski,¹⁷¹ K. Goulianos,¹⁷¹ C. Mesropian,¹⁷¹ A. Agapitos,¹⁷² J. P. Chou,¹⁷² Y. Gershtein,¹⁷² T. A. Gómez Espinosa,¹⁷²
 E. Halkiadakis,¹⁷² M. Heindl,¹⁷² E. Hughes,¹⁷² S. Kaplan,¹⁷² R. Kunnawalkam Elayavalli,¹⁷² S. Kyriacou,¹⁷² A. Lath,¹⁷²
 R. Montalvo,¹⁷² K. Nash,¹⁷² M. Osherson,¹⁷² H. Saka,¹⁷² S. Salur,¹⁷² S. Schnetzer,¹⁷² D. Sheffield,¹⁷² S. Somalwar,¹⁷²
 R. Stone,¹⁷² S. Thomas,¹⁷² P. Thomassen,¹⁷² M. Walker,¹⁷² A. G. Delannoy,¹⁷³ J. Heideman,¹⁷³ G. Riley,¹⁷³ K. Rose,¹⁷³
 S. Spanier,¹⁷³ K. Thapa,¹⁷³ O. Bouhali,^{174,ttt} A. Castaneda Hernandez,^{174,ttt} A. Celik,¹⁷⁴ M. Dalchenko,¹⁷⁴ M. De Mattia,¹⁷⁴
 A. Delgado,¹⁷⁴ S. Dildick,¹⁷⁴ R. Eusebi,¹⁷⁴ J. Gilmore,¹⁷⁴ T. Huang,¹⁷⁴ T. Kamon,^{174,uuu} R. Mueller,¹⁷⁴ Y. Pakhotin,¹⁷⁴
 R. Patel,¹⁷⁴ A. Perloff,¹⁷⁴ L. Perniè,¹⁷⁴ D. Rathjens,¹⁷⁴ A. Safonov,¹⁷⁴ A. Tatarinov,¹⁷⁴ K. A. Ulmer,¹⁷⁴ N. Akchurin,¹⁷⁵
 J. Damgov,¹⁷⁵ F. De Guio,¹⁷⁵ P. R. Duderø,¹⁷⁵ J. Faulkner,¹⁷⁵ E. Gурpinar,¹⁷⁵ S. Kunori,¹⁷⁵ K. Lamichhane,¹⁷⁵ S. W. Lee,¹⁷⁵
 T. Mengke,¹⁷⁵ S. Muthumuni,¹⁷⁵ T. Peltola,¹⁷⁵ S. Undleeb,¹⁷⁵ I. Volobouev,¹⁷⁵ Z. Wang,¹⁷⁵ S. Greene,¹⁷⁶ A. Gurrola,¹⁷⁶
 R. Janjam,¹⁷⁶ W. Johns,¹⁷⁶ C. Maguire,¹⁷⁶ A. Melo,¹⁷⁶ H. Ni,¹⁷⁶ K. Padeken,¹⁷⁶ P. Sheldon,¹⁷⁶ S. Tuo,¹⁷⁶ J. Velkovska,¹⁷⁶
 Q. Xu,¹⁷⁶ M. W. Arenton,¹⁷⁷ P. Barria,¹⁷⁷ B. Cox,¹⁷⁷ R. Hirosky,¹⁷⁷ M. Joyce,¹⁷⁷ A. Ledovskoy,¹⁷⁷ H. Li,¹⁷⁷ C. Neu,¹⁷⁷
 T. Sinthuprasith,¹⁷⁷ Y. Wang,¹⁷⁷ E. Wolfe,¹⁷⁷ F. Xia,¹⁷⁷ R. Harr,¹⁷⁸ P. E. Karchin,¹⁷⁸ N. Poudyal,¹⁷⁸ J. Sturdy,¹⁷⁸ P. Thapa,¹⁷⁸
 S. Zaleski,¹⁷⁸ M. Brodski,¹⁷⁹ J. Buchanan,¹⁷⁹ C. Caillol,¹⁷⁹ D. Carlsmith,¹⁷⁹ S. Dasu,¹⁷⁹ L. Dodd,¹⁷⁹ S. Duric,¹⁷⁹
 B. Gombor,¹⁷⁹ M. Grothe,¹⁷⁹ M. Herndon,¹⁷⁹ A. Hervé,¹⁷⁹ U. Hussain,¹⁷⁹ P. Klabbers,¹⁷⁹ A. Lanaro,¹⁷⁹ A. Levine,¹⁷⁹
 K. Long,¹⁷⁹ R. Loveless,¹⁷⁹ V. Rekovic,¹⁷⁹ T. Ruggles,¹⁷⁹ A. Savin,¹⁷⁹ N. Smith,¹⁷⁹ W. H. Smith,¹⁷⁹ and N. Woods¹⁷⁹

(CMS Collaboration)

¹*Yerevan Physics Institute, Yerevan, Armenia*

²*Institut für Hochenergiephysik, Wien, Austria*

³*Institute for Nuclear Problems, Minsk, Belarus*

⁴*Universiteit Antwerpen, Antwerpen, Belgium*

⁵*Vrije Universiteit Brussel, Brussel, Belgium*

⁶*Université Libre de Bruxelles, Bruxelles, Belgium*

⁷*Ghent University, Ghent, Belgium*

⁸*Université Catholique de Louvain, Louvain-la-Neuve, Belgium*

⁹*Centro Brasileiro de Pesquisas Físicas, Rio de Janeiro, Brazil*

¹⁰*Universidade do Estado do Rio de Janeiro, Rio de Janeiro, Brazil*

^{11a}*Universidade Estadual Paulista, São Paulo, Brazil*

^{11b}*Universidade Federal do ABC, São Paulo, Brazil*

¹²*Institute for Nuclear Research and Nuclear Energy, Bulgarian Academy of Sciences, Sofia, Bulgaria*

¹³*University of Sofia, Sofia, Bulgaria*

¹⁴*Beihang University, Beijing, China*

¹⁵*Institute of High Energy Physics, Beijing, China*

¹⁶*State Key Laboratory of Nuclear Physics and Technology, Peking University, Beijing, China*

¹⁷*Tsinghua University, Beijing, China*

¹⁸*Universidad de Los Andes, Bogota, Colombia*

¹⁹*University of Split, Faculty of Electrical Engineering, Mechanical Engineering and Naval Architecture, Split, Croatia*

²⁰*University of Split, Faculty of Science, Split, Croatia*

²¹*Institute Rudjer Boskovic, Zagreb, Croatia*

²²*University of Cyprus, Nicosia, Cyprus*

²³*Charles University, Prague, Czech Republic*

²⁴*Universidad San Francisco de Quito, Quito, Ecuador*

²⁵*Academy of Scientific Research and Technology of the Arab Republic of Egypt, Egyptian Network of High Energy Physics, Cairo, Egypt*

²⁶*National Institute of Chemical Physics and Biophysics, Tallinn, Estonia*

²⁷*Department of Physics, University of Helsinki, Helsinki, Finland*

²⁸*Helsinki Institute of Physics, Helsinki, Finland*

- ²⁹Lappeenranta University of Technology, Lappeenranta, Finland
³⁰IRFU, CEA, Université Paris-Saclay, Gif-sur-Yvette, France
³¹Laboratoire Leprince-Ringuet, Ecole polytechnique, CNRS/IN2P3, Université Paris-Saclay, Palaiseau, France
³²Université de Strasbourg, CNRS, IPHC UMR 7178, F-67000 Strasbourg, France
³³Centre de Calcul de l'Institut National de Physique Nucléaire et de Physique des Particules, CNRS/IN2P3, Villeurbanne, France
³⁴Université de Lyon, Université Claude Bernard Lyon 1, CNRS-IN2P3, Institut de Physique Nucléaire de Lyon, Villeurbanne, France
³⁵Georgian Technical University, Tbilisi, Georgia
³⁶Tbilisi State University, Tbilisi, Georgia
³⁷RWTH Aachen University, I. Physikalisches Institut, Aachen, Germany
³⁸RWTH Aachen University, III. Physikalisches Institut A, Aachen, Germany
³⁹RWTH Aachen University, III. Physikalisches Institut B, Aachen, Germany
⁴⁰Deutsches Elektronen-Synchrotron, Hamburg, Germany
⁴¹University of Hamburg, Hamburg, Germany
⁴²Institut für Experimentelle Kernphysik, Karlsruhe, Germany
⁴³Institute of Nuclear and Particle Physics (INPP), NCSR Demokritos, Aghia Paraskevi, Greece
⁴⁴National and Kapodistrian University of Athens, Athens, Greece
⁴⁵National Technical University of Athens, Athens, Greece
⁴⁶University of Ioánnina, Ioánnina, Greece
⁴⁷MTA-ELTE Lendület CMS Particle and Nuclear Physics Group, Eötvös Loránd University, Budapest, Hungary
⁴⁸Wigner Research Centre for Physics, Budapest, Hungary
⁴⁹Institute of Nuclear Research ATOMKI, Debrecen, Hungary
⁵⁰Institute of Physics, University of Debrecen, Debrecen, Hungary
⁵¹Indian Institute of Science (IISc), Bangalore, India
⁵²National Institute of Science Education and Research, Bhubaneswar, India
⁵³Panjab University, Chandigarh, India
⁵⁴University of Delhi, Delhi, India
⁵⁵Saha Institute of Nuclear Physics, HBNI, Kolkata, India
⁵⁶Indian Institute of Technology Madras, Madras, India
⁵⁷Bhabha Atomic Research Centre, Mumbai, India
⁵⁸Tata Institute of Fundamental Research-A, Mumbai, India
⁵⁹Tata Institute of Fundamental Research-B, Mumbai, India
⁶⁰Indian Institute of Science Education and Research (IISER), Pune, India
⁶¹Institute for Research in Fundamental Sciences (IPM), Tehran, Iran
⁶²University College Dublin, Dublin, Ireland
^{63a}INFN Sezione di Bari, Bari, Italy
^{63b}Università di Bari, Bari, Italy
^{63c}Politecnico di Bari, Bari, Italy
^{64a}INFN Sezione di Bologna, Bologna, Italy
^{64b}Università di Bologna, Bologna, Italy
^{65a}INFN Sezione di Catania, Catania, Italy
^{65b}Università di Catania, Catania, Italy
^{66a}INFN Sezione di Firenze, Firenze, Italy
^{66b}Università di Firenze, Firenze, Italy
⁶⁷INFN Laboratori Nazionali di Frascati, Frascati, Italy
^{68a}INFN Sezione di Genova, Genova, Italy
^{68b}Università di Genova, Genova, Italy
^{69a}INFN Sezione di Milano-Bicocca
^{69b}Università di Milano-Bicocca
^{70a}INFN Sezione di Napoli, Napoli, Italy
^{70b}Università di Napoli 'Federico II', Napoli, Italy
^{70c}Università della Basilicata, Potenza, Italy
^{70d}Università G. Marconi, Roma, Italy
^{71a}INFN Sezione di Padova, Padova, Italy
^{71b}Università di Padova, Padova, Italy
^{71c}Università di Trento, Trento, Italy
^{72a}INFN Sezione di Pavia, Pavia, Italy
^{72b}Università di Pavia, Pavia, Italy
^{73a}INFN Sezione di Perugia, Perugia, Italy
^{73b}Università di Perugia, Perugia, Italy
^{74a}INFN Sezione di Pisa, Pisa, Italy

- ^{74b}Università di Pisa, Pisa, Italy
^{74c}Scuola Normale Superiore di Pisa, Pisa, Italy
^{75a}INFN Sezione di Roma, Rome, Italy
^{75b}Sapienza Università di Roma, Rome, Italy
^{76a}INFN Sezione di Torino, Torino, Italy
^{76b}Università di Torino, Torino, Italy
^{76c}Università del Piemonte Orientale, Novara, Italy
^{77a}INFN Sezione di Trieste, Trieste, Italy
^{77b}Università di Trieste, Trieste, Italy
⁷⁸Kyungpook National University, Daegu, Korea
⁷⁹Chonnam National University, Institute for Universe and Elementary Particles, Kwangju, Korea
⁸⁰Hanyang University, Seoul, Korea
⁸¹Korea University, Seoul, Korea
⁸²Seoul National University, Seoul, Korea
⁸³University of Seoul, Seoul, Korea
⁸⁴Sungkyunkwan University, Suwon, Korea
⁸⁵Vilnius University, Vilnius, Lithuania
⁸⁶National Centre for Particle Physics, Universiti Malaya, Kuala Lumpur, Malaysia
⁸⁷Centro de Investigación y de Estudios Avanzados del IPN, Mexico City, Mexico
⁸⁸Universidad Iberoamericana, Mexico City, Mexico
⁸⁹Benemerita Universidad Autónoma de Puebla, Puebla, Mexico
⁹⁰Universidad Autónoma de San Luis Potosí, San Luis Potosí, Mexico
⁹¹University of Auckland, Auckland, New Zealand
⁹²University of Canterbury, Christchurch, New Zealand
⁹³National Centre for Physics, Quaid-I-Azam University, Islamabad, Pakistan
⁹⁴National Centre for Nuclear Research, Swierk, Poland
⁹⁵Institute of Experimental Physics, Faculty of Physics, University of Warsaw, Warsaw, Poland
⁹⁶Laboratório de Instrumentação e Física Experimental de Partículas, Lisboa, Portugal
⁹⁷Joint Institute for Nuclear Research, Dubna, Russia
⁹⁸Petersburg Nuclear Physics Institute, Gatchina (St. Petersburg), Russia
⁹⁹Institute for Nuclear Research, Moscow, Russia
¹⁰⁰Institute for Theoretical and Experimental Physics, Moscow, Russia
¹⁰¹Moscow Institute of Physics and Technology, Moscow, Russia
¹⁰²National Research Nuclear University 'Moscow Engineering Physics Institute' (MEPhI), Moscow, Russia
¹⁰³P.N. Lebedev Physical Institute, Moscow, Russia
¹⁰⁴Skobeltsyn Institute of Nuclear Physics, Lomonosov Moscow State University, Moscow, Russia
¹⁰⁵Novosibirsk State University (NSU), Novosibirsk, Russia
¹⁰⁶State Research Center of Russian Federation, Institute for High Energy Physics of NRC "Kurchatov Institute", Protvino, Russia
¹⁰⁷National Research Tomsk Polytechnic University, Tomsk, Russia
¹⁰⁸University of Belgrade, Faculty of Physics and Vinca Institute of Nuclear Sciences, Belgrade, Serbia
¹⁰⁹Centro de Investigaciones Energéticas Medioambientales y Tecnológicas (CIEMAT), Madrid, Spain
¹¹⁰Universidad Autónoma de Madrid, Madrid, Spain
¹¹¹Universidad de Oviedo, Oviedo, Spain
¹¹²Instituto de Física de Cantabria (IFCA), CSIC-Universidad de Cantabria, Santander, Spain
¹¹³CERN, European Organization for Nuclear Research, Geneva, Switzerland
¹¹⁴Paul Scherrer Institut, Villigen, Switzerland
¹¹⁵ETH Zurich—Institute for Particle Physics and Astrophysics (IPA), Zurich, Switzerland
¹¹⁶Universität Zürich, Zurich, Switzerland
¹¹⁷National Central University, Chung-Li, Taiwan
¹¹⁸National Taiwan University (NTU), Taipei, Taiwan
¹¹⁹Chulalongkorn University, Faculty of Science, Department of Physics, Bangkok, Thailand
¹²⁰Çukurova University, Physics Department, Science and Art Faculty, Adana, Turkey
¹²¹Middle East Technical University, Physics Department, Ankara, Turkey
¹²²Bogazici University, Istanbul, Turkey
¹²³Istanbul Technical University, Istanbul, Turkey
¹²⁴Institute for Scintillation Materials of National Academy of Science of Ukraine, Kharkov, Ukraine
¹²⁵National Scientific Center, Kharkov Institute of Physics and Technology, Kharkov, Ukraine
¹²⁶University of Bristol, Bristol, United Kingdom
¹²⁷Rutherford Appleton Laboratory, Didcot, United Kingdom
¹²⁸Imperial College, London, United Kingdom

- ¹²⁹*Brunel University, Uxbridge, United Kingdom*
¹³⁰*Baylor University, Waco, Texas, USA*
¹³¹*Catholic University of America, Washington, DC, USA*
¹³²*The University of Alabama, Tuscaloosa, Alabama, USA*
¹³³*Boston University, Boston, Massachusetts, USA*
¹³⁴*Brown University, Providence, Rhode Island, USA*
¹³⁵*University of California, Davis, Davis, California, USA*
¹³⁶*University of California, Los Angeles, California, USA*
¹³⁷*University of California, Riverside, Riverside, California, USA*
¹³⁸*University of California, San Diego, La Jolla, California, USA*
¹³⁹*University of California, Santa Barbara—Department of Physics, Santa Barbara, California, USA*
¹⁴⁰*California Institute of Technology, Pasadena, California, USA*
¹⁴¹*Carnegie Mellon University, Pittsburgh, Pennsylvania, USA*
¹⁴²*University of Colorado Boulder, Boulder, Colorado, USA*
¹⁴³*Cornell University, Ithaca, New York, USA*
¹⁴⁴*Fermi National Accelerator Laboratory, Batavia, Illinois, USA*
¹⁴⁵*University of Florida, Gainesville, Florida, USA*
¹⁴⁶*Florida International University, Miami, Florida, USA*
¹⁴⁷*Florida State University, Tallahassee, Florida, USA*
¹⁴⁸*Florida Institute of Technology, Melbourne, Florida, USA*
¹⁴⁹*University of Illinois at Chicago (UIC), Chicago, Illinois, USA*
¹⁵⁰*The University of Iowa, Iowa City, Iowa, USA*
¹⁵¹*Johns Hopkins University, Baltimore, Maryland, USA*
¹⁵²*The University of Kansas, Lawrence, Kansas, USA*
¹⁵³*Kansas State University, Manhattan, Kansas, USA*
¹⁵⁴*Lawrence Livermore National Laboratory, Livermore, California, USA*
¹⁵⁵*University of Maryland, College Park, Maryland, USA*
¹⁵⁶*Massachusetts Institute of Technology, Cambridge, Massachusetts, USA*
¹⁵⁷*University of Minnesota, Minneapolis, Minnesota, USA*
¹⁵⁸*University of Mississippi, Oxford, Mississippi, USA*
¹⁵⁹*University of Nebraska-Lincoln, Lincoln, Nebraska, USA*
¹⁶⁰*State University of New York at Buffalo, Buffalo, New York, USA*
¹⁶¹*Northeastern University, Boston, Massachusetts, USA*
¹⁶²*Northwestern University, Evanston, Illinois, USA*
¹⁶³*University of Notre Dame, Notre Dame, Indiana, USA*
¹⁶⁴*The Ohio State University, Columbus, Ohio, USA*
¹⁶⁵*Princeton University, Princeton, New Jersey, USA*
¹⁶⁶*University of Puerto Rico, Mayaguez, Puerto Rico*
¹⁶⁷*Purdue University, West Lafayette, Indiana, USA*
¹⁶⁸*Purdue University Northwest, Hammond, Indiana, USA*
¹⁶⁹*Rice University, Houston, Texas, USA*
¹⁷⁰*University of Rochester, Rochester, New York, USA*
¹⁷¹*The Rockefeller University, New York, USA*
¹⁷²*Rutgers, The State University of New Jersey, Piscataway, New Jersey, USA*
¹⁷³*University of Tennessee, Knoxville, Tennessee, USA*
¹⁷⁴*Texas A&M University, College Station, Texas, USA*
¹⁷⁵*Texas Tech University, Lubbock, Texas, USA*
¹⁷⁶*Vanderbilt University, Nashville, Tennessee, USA*
¹⁷⁷*University of Virginia, Charlottesville, Virginia, USA*
¹⁷⁸*Wayne State University, Detroit, Michigan, USA*
¹⁷⁹*University of Wisconsin—Madison, Madison, Wisconsin, USA*

^aDeceased.

^bAlso at Vienna University of Technology, Vienna, Austria.

^cAlso at IRFU, CEA, Université Paris-Saclay, Gif-sur-Yvette, France.

^dAlso at Universidade Estadual de Campinas, Campinas, Brazil.

^eAlso at Federal University of Rio Grande do Sul, Porto Alegre, Brazil.

^fAlso at Université Libre de Bruxelles, Bruxelles, Belgium.

^gAlso at Institute for Theoretical and Experimental Physics, Moscow, Russia.

^hAlso at Joint Institute for Nuclear Research, Dubna, Russia.

- ⁱ Also at Ain Shams University, Cairo, Egypt.
- ^j Also at Cairo University, Cairo, Egypt.
- ^k Also at British University in Egypt, Cairo, Egypt.
- ^l Also at Fayoum University, El-Fayoum, Egypt.
- ^m Also at Department of Physics, King Abdulaziz University, Jeddah, Saudi Arabia.
- ⁿ Also at Université de Haute Alsace, Mulhouse, France.
- ^o Also at Skobeltsyn Institute of Nuclear Physics, Lomonosov Moscow State University, Moscow, Russia.
- ^p Also at Tbilisi State University, Tbilisi, Georgia.
- ^q Also at CERN, European Organization for Nuclear Research, Geneva, Switzerland.
- ^r Also at RWTH Aachen University, III. Physikalisches Institut A, Aachen, Germany.
- ^s Also at University of Hamburg, Hamburg, Germany.
- ^t Also at Brandenburg University of Technology, Cottbus, Germany.
- ^u Also at MTA-ELTE Lendület CMS Particle and Nuclear Physics Group, Eötvös Loránd University, Budapest, Hungary.
- ^v Also at Institute of Nuclear Research ATOMKI, Debrecen, Hungary.
- ^w Also at Institute of Physics, University of Debrecen, Debrecen, Hungary.
- ^x Also at IIT Bhubaneswar, Bhubaneswar, India.
- ^y Also at Institute of Physics, Bhubaneswar, India.
- ^z Also at Shoolini University, Solan, India.
- ^{aa} Also at University of Visva-Bharati, Santiniketan, India.
- ^{bb} Also at University of Ruhuna, Matara, Sri Lanka.
- ^{cc} Also at Isfahan University of Technology, Isfahan, Iran.
- ^{dd} Also at Yazd University, Yazd, Iran.
- ^{ee} Also at Plasma Physics Research Center, Science and Research Branch, Islamic Azad University, Tehran, Iran.
- ^{ff} Also at Università degli Studi di Siena, Siena, Italy.
- ^{gg} Also at INFN Sezione di Milano-Bicocca, Università di Milano-Bicocca, Milano, Italy.
- ^{hh} Also at International Islamic University of Malaysia, Kuala Lumpur, Malaysia.
- ⁱⁱ Also at Malaysian Nuclear Agency, MOSTI, Kajang, Malaysia.
- ^{jj} Also at Consejo Nacional de Ciencia y Tecnología, Mexico city, Mexico.
- ^{kk} Also at Warsaw University of Technology, Institute of Electronic Systems, Warsaw, Poland.
- ^{ll} Also at National Research Nuclear University 'Moscow Engineering Physics Institute' (MEPhI), Moscow, Russia.
- ^{mm} Also at Institute for Nuclear Research, Moscow, Russia.
- ⁿⁿ Also at St. Petersburg State Polytechnical University, St. Petersburg, Russia.
- ^{oo} Also at University of Florida, Gainesville, Florida, USA.
- ^{pp} Also at P.N. Lebedev Physical Institute, Moscow, Russia.
- ^{qq} Also at Budker Institute of Nuclear Physics, Novosibirsk, Russia.
- ^{rr} Also at Faculty of Physics, University of Belgrade, Belgrade, Serbia.
- ^{ss} Also at University of Belgrade, Faculty of Physics and Vinca Institute of Nuclear Sciences, Belgrade, Serbia.
- ^{tt} Also at Scuola Normale e Sezione dell'INFN, Pisa, Italy.
- ^{uu} Also at National and Kapodistrian University of Athens, Athens, Greece.
- ^{vv} Also at Riga Technical University, Riga, Latvia.
- ^{ww} Also at Universität Zürich, Zurich, Switzerland.
- ^{xx} Also at Stefan Meyer Institute for Subatomic Physics.
- ^{yy} Also at Gaziosmanpasa University, Tokat, Turkey.
- ^{zz} Also at Istanbul Aydin University, Istanbul, Turkey.
- ^{aaa} Also at Mersin University, Mersin, Turkey.
- ^{bbb} Also at Piri Reis University, Istanbul, Turkey.
- ^{ccc} Also at Adiyaman University, Adiyaman, Turkey.
- ^{ddd} Also at Izmir Institute of Technology, Izmir, Turkey.
- ^{eee} Also at Necmettin Erbakan University, Konya, Turkey.
- ^{fff} Also at Marmara University, Istanbul, Turkey.
- ^{ggg} Also at Kafkas University, Kars, Turkey.
- ^{hhh} Also at Istanbul Bilgi University, Istanbul, Turkey.
- ⁱⁱⁱ Also at Rutherford Appleton Laboratory, Didcot, United Kingdom.
- ^{jjj} Also at School of Physics and Astronomy, University of Southampton, Southampton, United Kingdom.
- ^{kkk} Also at Monash University, Faculty of Science, Clayton, Australia.
- ^{lll} Also at Instituto de Astrofísica de Canarias, La Laguna, Spain.
- ^{mmm} Also at Utah Valley University, Orem, Utah, USA.
- ⁿⁿⁿ Also at Purdue University, West Lafayette, Indiana, USA.
- ^{ooo} Also at Beykent University.
- ^{ppp} Also at Bingol University, Bingol, Turkey.

^{qqq}Also at Erzincan University, Erzincan, Turkey.

^{rrr}Also at Sinop University, Sinop, Turkey.

^{sss}Also at Mimar Sinan University, Istanbul, Istanbul, Turkey.

^{ttt}Also at Texas A&M University at Qatar, Doha, Qatar.

^{uuu}Also at Kyungpook National University, Daegu, Korea.